Viscosity of a Room Temperature Ionic Liquid: Predictions from Nonequilibrium and Equilibrium Molecular Dynamics Simulations

Oleg Borodin,*,†,‡ Grant D. Smith,† and Hojin Kim†

Department of Materials Science & Engineering, 122 South Central Campus Drive, Room 304, University of Utah, Salt Lake City, Utah 84112-0560, and Wasatch Molecular Inc., 2141 St. Mary's Drive, Suite 102, Salt Lake City, Utah 84108

Received: November 13, 2008; Revised Manuscript Received: January 23, 2009

Nonequilibrium molecular dynamics (NEMD) simulations have been performed on 1-methyl-3-ethylimidazolium bis(trifluoromethane)sulfonimide [emim][Ntf_2] using Lees−Edwards boundary conditions. A range of inverse shear rates corresponding to a fraction of the rotational relaxation time for the slowest relaxing molecular axis of anion and cation to 20 rotational relaxation times ($1/20\ \tau_{rot} < \dot{\gamma} < 5/\tau_{rot}$) has been investigated. An extrapolation of the shear-rate-dependent viscosity obtained from these simulations to zero shear rate using the empirical three-parameter Carreau equation yielded excellent agreement with the viscosity obtained from equilibrium MD simulations. Based upon the Carreau equation fit to the simulation data, shear-thinning behavior was observed in [emim][Ntf_2] for all shear rates investigated, implying that Newtonian behavior is observed in [emim][Ntf_2] only for shear rates significantly lower than the inverse rotational relaxation time. A close resemblance between the apparent time-dependent viscosity extracted from equilibrium MD simulations and the shear-rate-dependent viscosity extracted from NEMD simulations has been found and discussed. MD simulations accurately predicted [emim][Ntf_2] density, self-diffusion coefficients, heat of vaporization, and lattice parameters for the crystalline phase.

I. Introduction

Room temperature ionic liquids (IL) have attracted significant attention from the scientific and business community over the past decade and have been widely investigated[1] for a variety of applications. The negligible vapor pressure, good thermal and electrochemical stability, good dissolution properties with many organic and inorganic compounds, low flammability,[2] and a wide variety of possible anions and cations are a few examples of characteristics that make ILs attractive for many applications. Molecular dynamics (MD) simulations are emerging as a powerful tool for reliable prediction of various properties of ILs. Indeed, most structural, thermodynamic, and transport properties of ILs are accessible from simulations. [1−11]

Viscosity is one of important properties of ILs for many existing and envisioned applications. [3,4] Because viscosity is a collective property of the system, and because many ILs have relatively high viscosity compared to organic solvents, accurate prediction of viscosity of ILs from MD simulations is computationally challenging. A limited number of MD simulations report viscosity predictions for ILs.[3,5−9] Maginn's group[3,4] has utilized reserve nonequilibrium molecular dynamics (RNEMD) to predict viscosity of [1-methyl-ethyl-3-methylimidazolium-][bis(trifluoromethane)sulfonamide], or [emim][Ntf_2], as a function of shear rate and temperature. In this method, a momentum flux is imposed on the simulated IL and the velocity gradient is measured allowing one to calculate shear-rate-dependent viscosity. They found very good agreement between predicted viscosity and experimental data. RNEMD and equilibrium MD simulations of [emim][PF_6] by Wei et al.[10] demonstrated good agreement between viscosity extracted between RNEMD and equilibrium MD simulations. Several other groups have reported viscosity of ILs from equilibrium simulations using Einstein or Green−Kubo methods.[6,8,11−13] The wave-vector-dependent viscosity was also reported (using transverse current)[5] with a significant dependence on the IL simulation box size.[7,14] The Ludwig group has reported the most accurate description of thermodynamics and transport properties (including viscosity) of [emim][Ntf_2] IL from equilibrium MD simulations.[9]

NEMD methods for predicting viscosity are typically employed at very high shear rate in order to obtain adequate signal (shear stress) to noise (stress fluctuations) ratio and to access reasonable shear strains (on the order of unity or greater) on time scales accessible to the simulations.[15−17] As a result, the inverse shear rates employed in NEMD simulations correspond to the time scale of molecular relaxation (e.g., rotational relaxation times). Hence, NEMD simulations largely probe the shear-thinning, non-Newtonian regime for the IL, and prediction of the shear-rate-independent viscosity in the Newtonian regime requires extrapolation to lower shear rates. In this work, we report on a study of the shear-rate-dependent behavior of the viscosity of [emim][Ntf_2] from NEMD simulations and compare extrapolated viscosity with that obtained from (zero-shear-rate) equilibrium MD simulations. Emphasis is placed on the influence of the extrapolation procedure of strain-rate-dependent viscosity on predicted low strain rate viscosity, the shear strain rate at which the transition from shear-thinning to Newtonian behavior occurs, and the relationship between this transition and molecular relaxation times.

II. Molecular Dynamics Simulations Methodology

A version of the MD simulation package *Lucretius* that includes many-body polarization was used for all MD simula-

* To whom correspondence should be addressed. E-mail: Oleg.Borodin@utah.edu.
† University of Utah.
‡ Wasatch Molecular Inc.

10.1021/jp810016e CCC: $40.75
Published on Web 03/10/2009

tions.[18] A quantum chemistry-based, all atom, dipole polarizable potential of similar form to that utilized in our previous studies of RTILs[12,13,19] was used in this work. Force field parameters are available from Wasatch Molecular Inc. upon request.[20] Force field functional form and development methodology are discussed in the Supporting Information, where we demonstrate that the developed force field predicts [emim][Ntf_2] density, self-diffusion coefficients, heat of vaporization, and lattice parameters for the crystalline phase in excellent agreement with available experimental data.

A three-dimensional, periodic cubic simulation cell consisting of 150 [emim][Ntf_2] ion pairs was simulated. The IL was created in the gas phase corresponding to a cell (linear) dimension of approximately 75 Å. The dimensions of the simulation cells were reduced to yield estimated densities at 393 K followed by a 0.8 ns NPT run. The average box size from the NPT run was utilized in the 20 ns NVT run at 393 K. MD simulations at 333 and 298 K were performed for 7−10 ns utilizing the average box sizes from 1 ns NPT equilibration runs.

The Ewald summation method was used for electrostatic interactions between partial charges with partial charges and partial charges with induced dipole moments. The Thole screening parameter[19] a_T, defining the width of the smeared charge distribution preventing polarization catastrophe from occurring, was set to 0.2. The interaction between an induced dipole and a partial charge separated by 3 bonds was scaled by 0.8, providing an improved description of the electrostatic potential around the molecules. Multiple time step integration with an inner time step of 0.5 fs (bonded interactions), a central time step of 1.5 fs for all nonbonded interactions within a truncation of 7.0 Å, and an outer time step of 3.0 fs for all nonbonded between 7.0 Å and the nonbonded truncation distance of 10.5 Å as well as for the reciprocal part of Ewald was employed. A Nose−Hoover thermostat (NPT and NVT simulations) and a barostat (NPT simulations) were used to control the temperature and pressure with the associated frequencies of 10^{-2} and 0.5×10^{-3} fs.

The equilibrium (zero-shear-rate) viscosity was calculated using the Einstein relation including both diagonal and nondiagonal elements to enhance statistics[21−23]

$$\eta = \lim_{t\to\infty} \eta(t) = \lim_{t\to\infty} \frac{V}{20k_B T t}\langle \sum_{\alpha,\beta} (L_{\alpha\beta}(t) - L_{\alpha\beta}(0))^2 \rangle \quad (1)$$

where $L_{\alpha\beta}(t) = \int_0^t P_{\alpha\beta}(t')\, dt'$, k_B is the Boltzmann constant, T is temperature, t is time, V is the volume of the simulation box, and $P_{\alpha\beta}$ is the symmeterized and traceless stress sensor given by

$$P_{\alpha\beta} = \omega_{\alpha\beta}\left(\frac{\sigma_{\alpha\beta} + \sigma_{\beta\alpha}}{2} - \frac{\delta_{\alpha\beta}}{3}\mathrm{tr}(\sigma)\right) \quad (2)$$

where $\sigma_{\alpha\beta}$ is the stress tensor, $\omega_{\alpha\beta} = 1$ for $\alpha \neq \beta$, $\omega_{\alpha\beta} = 4/3$ for $\alpha = \beta$, $\delta_{\alpha\beta} = 1$ for $\alpha = \beta$, and $\delta_{\alpha\beta} = 0$ for $\alpha \neq \beta$.

The Lees−Edwards boundary conditions have been implemented in the Lucretius code as outlined in Wheeler et al.[16] NEMD simulations were performed on IL containing the same number of ions and using the same density at 393 K as a function of shear rate. The simulation lengths were 1.0−6 ns with shorted trajectories used for higher rates. Unlike the RNEMD and transverse current methods for determining viscosity discussed above, which yield a system-size-dependent viscosity because the minimum k-vector allowable is determined by the dimensions of the simulation cell, NEMD using Lees−Edwards boundary conditions yield the viscosity in the limit of $k = 0$.[24]

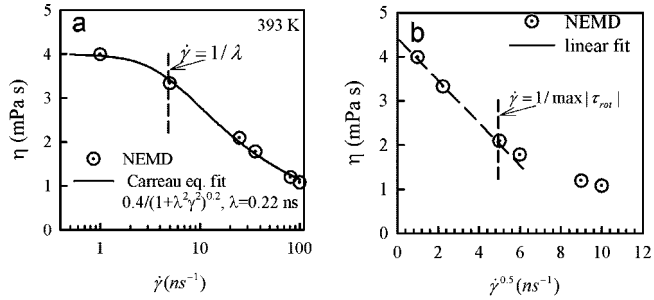

Figure 1. Shear-rate-dependent viscosity of [emim][Ntf_2] at 393 K from NEMD using Lees−Edwards boundary conditions.

III. Results and Discussion

Shear-Rate-Dependent Viscosity and Rotational Relaxation. The shear-rate-dependent viscosity from NEMD simulations of [emim][Ntf_2] using Lees−Edwards boundary conditions is shown in Figure 1a. Clear shear-thinning behavior is observed at high shear rates in accord with previous reports.[3,10] From the data alone, it is not possible to determine if the lowest shear rate ($\dot{\gamma} = 1$ ns^{-1}) investigated lies in the Newtonian regime. The NEMD data was fitted with Carreau equation[3]

$$\eta(\dot{\gamma}) = \eta_0^{-1}(1 + (\lambda\dot{\gamma})^2)^{-p} \quad (3)$$

where η_0 is the zero-shear value of viscosity (Newtonian viscosity), λ is the characteristic time constant, and p is an exponent. The fitted parameters are shown in Figure 1a. The value for the exponent $p = 0.2$ is similar to the value of 0.28 obtained for [emim][PF_6] obtained in previous RNEMD simulations.[10] In order for Newtonian behavior to be observed according to the Carreau equation, $\lambda^*\dot{\gamma}$ must be significantly smaller than 1, yielding $\dot{\gamma}$ (Newtonian) $\ll 1/\lambda \approx 5$ ns^{-1}. Hence, at $\dot{\gamma} = 1/\lambda$, the material still experiences significant shear thinning as can be seen in Figure 1a. Newtonian behavior is not observed in Figure 1a until $\dot{\gamma} \approx 1$ ns^{-1}, corresponding to time scales of around 1 ns, about 5 times longer than the time constant obtained from the Carreau equation.

It is claimed[3,17,21,25] that the time scale for the onset of shear-thinning behavior in molecular liquids is closely related to the rotational relaxation time of the molecules. In order to examine this relationship for [emim][Ntf_2], we have calculated rotational relaxation for both $emim^+$ and Ntf_2^- by fixing an coordinate system in the imidazolium ring and to S−N−S bend in Ntf_2^- as was described previously.[12] The relaxation times (τ_{rot}) for $emim^+$ range from 0.017 to 0.047 ns and from 0.015 to 0.049 ns for Ntf_2^- depending the chosen axis at 393 K. Taking the longest rotational relaxation time yields a corresponding shear rate of $\dot{\gamma} = 1/\tau_{rot} \approx 20$ ns^{-1}, as shown in Figure 1a. This shear rate is somewhat greater than the rate associated with $1/\lambda = 4.5$ ns^{-1} and clearly is lies within the shear -thinning regime. Newtonian behavior is not observed in [emim][Ntf_2] until $\gamma < 1/10\tau_{rot}$.

Dependence of the Estimated Zero-Shear-Rate Viscosity on the Extrapolation Procedure. Maginn's group[3] has suggested that because of the low signal-to-noise ratio in NEMD simulations at low shear rates it is more accurate to estimate the zero-shear-rate viscosity based upon a linear extrapolation of $\eta(\dot{\gamma})$ vs $\dot{\gamma}^{0.5}$ than to use the Carreau equation, which is

sensitive to uncertainty in low-shear-rate data used in the fitting procedure. This same approach has been utilized by others for estimating the zero-shear-rate viscosity of nonioinic liquids.[16] Maginn advocates extrapolation of $\eta(\dot{\gamma})$ vs $\dot{\gamma}^{0.5}$ to a finite value of $\dot{\gamma}$ instead of extrapolation of $\eta(\dot{\gamma})$ to $\dot{\gamma} = 0$, as the later extrapolation is expected to result in overestimation of the viscosity. The viscosity of [emim][Ntf$_2$] from our NEMD simulations is plotted vs $\dot{\gamma}^{0.5}$ is Figure 1b showing that the linear extrapolation to $\dot{\gamma} = 0$ indeed results in overestimation of the viscosity by about 0.2 mPa s compared to the Carreau equation fit as well as the value obtained by equilibrium MD simulations (see below). However, the overestimation based on this extrapolation is only about 5% of the viscosity value. The linear fit shown in Figure 1b also suggest that only data at shear rates lower than $1/\max|\tau_{rot}|$ corresponding to $\dot{\gamma}^{0.5} = 4.8$ ns$^{-0.5}$ should be included in the fit. If a linear fit is made to three data points with the shear rate higher than $\dot{\gamma}^{0.5} > \max|\tau_{rot}|$ for $\dot{\gamma}^{0.5} > 4.8$ ns$^{-0.5}$, one would obtain a zero-shear value of 2.7 mPa s based upon extrapolation to $\dot{\gamma} = 0$. We conclude that in order to perform an accurate extrapolation to zero shear rate one need to utilize several data points with $\dot{\gamma} < 1/\max|\tau_{rot}|$. Inclusion of higher shear-rate data in the fit will result in an underestimation of the viscosity. An advantage of the Carreau equation fit is that it is not necessary to determine which data to include in the fitting as the equation accurately describes the shear-rate-dependent viscosity over the entire range of shear rates investigated.

An additional problem utilizing the linear η vs $\dot{\gamma}^{0.5}$ procedure is to determine what finite value $\dot{\gamma}$ of to which to carry out the extrapolation. Clearly this should be the shear rate corresponding to the onset of shear-thinning behavior. Previous NEMD simulations of alkanes[17,26] suggested that the onset of the shear thinning occurs around $\dot{\gamma} = 1/\tau_{rot}$, where τ_{rot} is the Rouse time. However, one should note that at the shear rate $\dot{\gamma} = 1/\tau_{rot}$ the shear viscosity typically is slightly below the Newtonian viscosity. For example, in the case of *n*-hexadecane,[17] viscosity at $\dot{\gamma} = 1/\tau_{rot}$ was found approximately 20−30% below the Newtonian viscosity value. In our simulations of [emim][Ntf$_2$], viscosity at $\dot{\gamma} = \max|\tau_{rot}|$, yielding $\dot{\gamma}^{0.5} = 4.8$ ns$^{-0.5}$, is approximately 50% of the extrapolated Newtonian viscosity value as shown in Figure 1b. Based upon the behavior for [emim][Ntf$_2$] observed in Figure 1a, we recommend extrapolation to $\dot{\gamma} = (1/10)\tau_{rot} \approx 1$ ns^{-1}, yielding $\dot{\gamma}^{0.5} = 1$ ns$^{-0.5}$ as shown in Figure 1b.

It is instructive to compare our simulation results with results of the previous RNEMD simulations of [emim][Ntf$_2$].[3] The slowest rotational relaxation times for emim$^+$ reported by Maginn's group[3] are a factor of 2−3 longer than the slowest relaxation time found in this work (at 333 and 393 K), yet, unexpectedly, both Maginn's group and this work report a good agreement between viscosity from MD simulations and experimental data. This raises the question as to why quite different rotational relaxation times from two simulations yield similar viscosities. One of the reasons behind this inconsistency lies in the fact that Maginn's group has reported viscosity at $\dot{\gamma} = 1/\tau_{rot}$ as Newtonian viscosity, thus underestimating viscosity by a factor of 2 as seen from Figure 1. Thus, the corrected viscosities of [emim][Ntf$_2$] from Maginn's group are expected to be a factor of 2 higher than experimental data. Interestingly, there is a parallel between viscosity and heat of vaporization data reported at 298 K. Maginn's group reported heat of vaporization (H^{vap}) of 143 kJ/mol, which is higher than the value from this work of $H^{vap} = 127.1$ kJ/mol, which is slightly lower than three experimental values[9] of 134−136 kJ/mol but is similar to the value of 130.6 kJ/mol reported by Ludwig's group.[9] Santos et al.[27] has reported a much higher value of $H^{vap} = 159$ kJ/mol from MD simulations using the Padua group's force field. The transport properties from this work are in excellent agreement with those reported by Ludwig's group[9] and experiments as shown in the Supporting Information, which is consistent with a good agreement between H^{vap} from these MD simulations and experiments. As reported by Ludwig's group,[9] ion transport using Padua's force field is approximately an order of magnitude slower compared to experimental data, which is consistent with a dramatic overestimation of the heat of vaporization by Padua's force field. Maginn's force field only slightly overestimates heat of vaporization at 298 K, which is consistent with our proposition that [emim][Ntf$_2$] viscosity utilizing Maginn's force field is expected to be approximately a factor of 2 higher than experimental values.

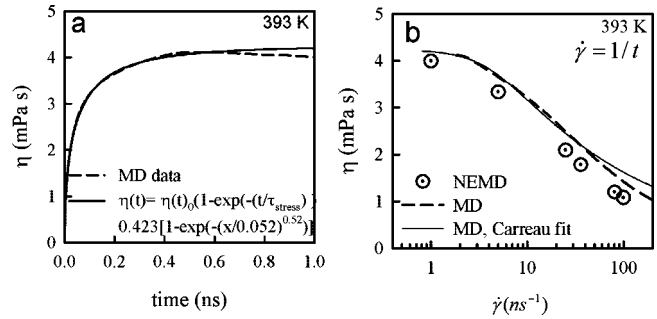

Figure 2. (a) Apparent viscosity $\eta(t)$ from equilibrium MD simulations of [emim][Ntf$_2$] at 393 K together with the fit to eq 5. (b) Apparent viscosity from equilibrium MD simulations plotted vs $(1/t)$ together with results from NEMD.

Viscosity from Equilibrium MD Simulations. The apparent viscosity $\eta(t)$ calculated from eqs 1−2 for [emim][Ntf$_2$] from our equilibrium MD simulations is shown in Figure 2. We take the plateau value of 4.23 mPa s as the viscosity, which is in excellent agreement with the value of 4.0 mPa s obtained from NEMD using Lees−Edwards boundary conditions as fit by the Carreau equation. The VTF fit to experimental data[28] from −10 to 100 °C yields a value of 4.46 mPa s. We confirmed that viscosity obtained from equilibrium MD simulations does not show dependence (within a few percent) on the length of the simulation run by analyzing the first 10 ns and the second 10 ns of the trajectory separately.

The shear stress autocorrelation function (ACF) $G(t)$ is often found to exhibit nonexponential behvaior for liquids[12] for times much larger than bond vibrations and can often be well described with a stretched exponential function

$$G(t) = G_0 \exp(-(t/\tau_{stress})^{\beta}) \quad (4)$$

where τ_{stress} is the characteristic stress decay time and the integral of eq 4 divided by G_0 is the shear stress relaxation time. Since the viscosity is the time integral of $G(t)$,[24,29] the apparent viscosity shown in Figure 2a should be well described by the functional form given by eq 5.

$$\eta(t) = \eta_0(1 - \exp(-(t/\tau_{stress})^{\beta}) \quad (5)$$

Indeed, Figure 2a shows a good representation of the apparent viscosity by eq 5. The resulting fitting parameters are also shown in Figure 2a. The shear stress relaxation time obtained as an integral of the stretched exponential fit to $G(t)$ is 0.097 ns, which

is similar in magnitude but 2 times higher than the longest rotational relaxation time for ions. Further exploration of the apparent viscosity versus time dependence indicates that that apparent viscosity value at $t = \tau_{rot}$ is about 2.8 mPa s, less than 4.23 mPa s extracted from the plateau value. There is a parallel between $\eta(t)$ extracted from equilibrium MD and $\eta(\dot{\gamma})$ extracted from NEMD simulations. The $\eta(t)$ reaches plateau at ~0.5 ns corresponding to $10\tau_{rot}$, while one need to extrapolate to $\dot{\gamma} \sim 1/(10\ \tau_{rot})$ to reach the end of the crossover regime from shear-thinning to Newtonian behavior. Moreover, when the apparent viscosity from MD simulations ($\eta^{MD}(\dot{\gamma})$) is plotted vs $\dot{\gamma} = 1/t$ as shown in Figure 2b, its behavior closely resembles the shear-rate dependence of viscosity extracted from NEMD simulations. It is indicative of the possibility of predicting the shear-thinning behavior of viscosity from equilibrium MD simulations in accord with the Cox−Merz rule that was observed to be valid for polymers.[30]

The apparent viscosity ($\eta^{MD}(\dot{\gamma})$) can also be fit with Carreau equation as shown in Figure 2b as was done for the shear-rate-dependent viscosity from NEMD simulations. Furthermore, analogously to utilizing the Carreau equation given by eq 1 or using the extrapolation of $\eta(\dot{\gamma})$ vs $\dot{\gamma}^{0.5}$, we suggest that one can adequately apply $\eta(\dot{\gamma})$ vs $\dot{\gamma}^{0.5}$ extrapolation to approximate the Newton value of viscosity for ILs from $\eta^{MD}(\dot{\gamma})$ in the same fashion as was discussed above for $\eta(\dot{\gamma})$ extracted from NEMD.

IV. Conclusions

NEMD simulations of [emim][Ntf_2] have been performed for a range of inverse shear rates corresponding to $1/20\ \tau_{rot} < \dot{\gamma} < 5/\tau_{rot}$, where τ_{rot} is the longest relaxation time of ions using force field that yields an excellent description of IL density, self-diffusion coefficients, heat of vaporization, and viscosity and lattice parameters for the crystal phase. An extrapolation of the shear-rate-dependent viscosity obtained from these simulations to zero shear rate using the empirical three-parameter Carreau equation yielded excellent agreement with the viscosity obtained from equilibrium MD simulations. Shear-thinning behavior was observed for shear rates $\dot{\gamma} > 0.1/\max|\tau_{rot}|$, implying that Newtonian behavior is observed in [emim][Ntf_2] IL only for shear rates significantly lower than the inverse rotational relaxation time. A close resemblance between the apparent viscosity $\eta^{MD}(\dot{\gamma})$ extracted from equilibrium MD simulations and the shear-rate-dependent viscosity $\eta(\dot{\gamma})$ extracted from NEMD simulations has been found. It is indicative of the possibility of predicting the shear-thinning behavior of viscosity from equilibrium MD simulations supporting the validity of the Cox−Merz rule for ionic liquids.

Acknowledgment. The authors are grateful for financial support of this work by Air Force Office of Scientific Research, Department of the Air Force contract number FA9550-08-C-003 to Wasatch Molecular Inc. and the U.S. Department of Energy under contract no. DE-AC02-05CH11231 on PO No. 6838611 to the University of Utah. Opinions, interpretations, conclusions, and recommendations are those of the authors and are not necessarily endorsed by the United States Air Force. An allocation of computer time from the Center for High Performance Computing at the University of Utah is gratefully acknowledged. G.S. acknowledges partial support from NSF MRSEC Grant DMR-1536145.

Supporting Information Available: Force field form, force field development methodology, [emim][Ntf_2] density, self-diffusion coefficients as a function of temperature, heat of vaporization, and lattice parameters for [emim][Ntf_2] crystal. This material is available free of charge via the Internet at http://pubs.acs.org.

References and Notes

(1) Smiglak, M.; Metlen, A.; Rogers, R. D. *Acc. Chem. Res.* **2007**, *40*, 1182.
(2) Fox, D. M.; Awad, W. H.; Gilman, J. W.; Maupin, P. H.; De Long, H. C.; Trulove, P. C. *Green Chem.* **2003**, *5*, 724.
(3) Kelkar, M. S.; Maginn, E. J. *J. Phys. Chem. B* **2007**, *111*, 4867.
(4) Maginn, E. J. *Acc. Chem. Res.* **2007**, *40*, 1200.
(5) Yan, T. Y.; Burnham, C. J.; Del Popolo, M. G.; Voth, G. A. *J. Phys. Chem. B* **2004**, *108*, 11877.
(6) Bhargava, B. L.; Balasubramanian, S. *J. Chem. Phys.* **2005**, *123*, 144505.
(7) Hu, Z.; Margulis, C. J. *Acc. Chem. Res.* **2007**, *40*, 1097.
(8) Schroder, C.; Wakai, C.; Weingartner, H.; Steinhauser, O. *J. Chem. Phys.* **2007**, *126*, 084511.
(9) Koddermann, T.; Paschek, D.; Ludwig, R. *Chem. Phys. Chem.* **2007**, *8*, 2464.
(10) Wei, Z.; Leroy, F.; Balasubramanian, S.; Muller-Plathe, F. *J. Phys. Chem. B* **2008**, *112*, 8129.
(11) Rey-Castro, C.; Vega, L. F. *J. Phys. Chem. B* **2006**, *110*, 14426.
(12) Borodin, O.; Smith, G. D. *J. Phys. Chem. B* **2006**, *110*, 11481.
(13) Borodin, O.; Smith, G. D.; Henderson, W. *J. Phys. Chem. B* **2006**, *110*, 16879.
(14) Hu, Z. H.; Margulis, C. J. *J. Phys. Chem. B* **2007**, *111*, 4705.
(15) McCabe, C.; Bedrov, D.; Borodin, O.; Smith, G. D.; Cummings, P. T. *Ind. Eng. Chem. Res.* **2003**, *42*, 6956.
(16) Wheeler, D. R.; Fuller, N. G.; Rowley, R. L. *Mol. Phys.* **1997**, *92*, 55.
(17) Tseng, H. C.; Wu, J. S.; Chang, R. Y. *J. Chem. Phys.* **2008**, *129*, 20.
(18) Ayyagari, C.; Bedrov, D.; Borodin, O.; Smith, G. D. Lucretius, MD simulation code http://www.eng.utah.edu/~gdsmith/lucretius.html.
(19) Borodin, O.; Smith, G. D. *J. Phys. Chem. B* **2006**, *110*, 6279.
(20) Borodin, O. APPLE&P (Atomistic Polarizable Potential for Liquids, Electrolytes and Polymers), rev 1e. www.wasatchmolecular.com.
(21) Daivis, P. J.; Evans, D. J. *J. Chem. Phys.* **1994**, *100*, 541.
(22) Mondello, M.; Grest, G. S. *J. Chem. Phys.* **1997**, *106*, 9327.
(23) Bedrov, D.; Smith, G. D.; Sewell, T. D. *J. Chem. Phys.* **2000**, *112*, 7203.
(24) Allen, M. P.; Tildesley, D. J. *Computer Simulation Of Liquids*; Oxford University Press: New York; 1987.
(25) Bair, S.; Winer, W. O. *Tribol. Lett.* **2007**, *26*, 223.
(26) Bair, S.; McCabe, C.; Cummings, P. T. *Phys. Rev. Lett.* **2002**, *88*, 058302.
(27) Santos, L. M. N. B. F.; Lopes, J. N. C.; Coutinho, J. A. P.; Esperanca, J. M. S. S.; Gomes, L. R.; Marrucho, I. M.; Rebelo, L. P. N. *J. Am. Chem. Soc.* **2007**, *129*, 284.
(28) Tokuda, H.; Hayamizu, K.; Ishii, K.; Susan, M. A. B. H.; Watanabe, M. *J. Phys. Chem. B* **2005**, *109*, 6103.
(29) Byutner, O.; Smith, G. D. *Macromolecules* **2002**, *35*, 3769.
(30) Kulicke, W. M.; Porter, R. S. *Rheol. Acta* **1980**, *19*, 601.

JP810016E